

Small and Medium Rings, 74¹⁾

Syntheses and Photoelectron Spectra of 7-Azanorbornadiene and Related Compounds

An Analysis with Fragment Orbitals

Hans-Josef Altenbach^{a*}, Dieter Constant^c, Hans-Dieter Martin^{a,b}, Bernhard Mayer^b, Monika Müller^b, and Emanuel Vogel^{a,c}

Fachbereich Chemie und Chemietechnik der Universität Gesamthochschule Paderborn^a, Warburger Straße 100, D-4790 Paderborn

Institut für Organische Chemie und Makromolekulare Chemie der Universität Düsseldorf^b, Universitätsstraße 1, D-4000 Düsseldorf

Institut für Organische Chemie der Universität Köln^c, Greinstraße 4, D-5000 Köln

Received August 13, 1990

Key Words: Lone-pair orientation / Lone pair interaction / Precanonical orbitals / Orbitals, localized / Calculations, ab initio STO-3G, MNDO, MM2 force field / PE Spectroscopy

The He(I) photoelectron spectra (PE) of 7-azanorbornane (**5**), 7-azanorbornene (**6**), and 7-azanorbornadiene (**7**) as well as of related urethanes have been recorded. The syntheses of these bicyclic compounds are described in detail. A most convenient analysis of the PE spectroscopic results is based on the procedure of Heilbronner-Schmelzer on an ab initio STO-3G level. This method allows to construct fragment orbitals elucidating the orientation of the nitrogen lone pair, the through-space interaction with π bonds, and the participation of σ bond orbitals. The result is remarkable: whereas the direct interaction of localized lone-pair and π orbitals is significant in both *syn*- and *anti*-orientation, the interaction of a localized

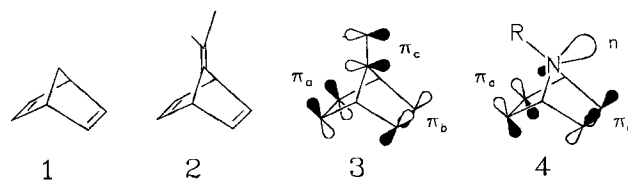
lone pair with a precanonical fragment π orbital is completely different in the two geometries. In **6-syn** a considerable interaction matrix element $F_{\psi_{np},\pi}^{syn} = -0.71$ eV comes to the fore, whereas the corresponding parameter in **6-anti** turns out to be almost zero, $F_{\psi_{np},\pi}^{anti} = +0.09$ eV. Since **6-syn** is calculated to be more stable than **6-anti**, it is this invertomer, **6-syn**, which is likely to be responsible for the main bands in the PE spectrum of **6**. The comparatively large experimental split between the first two PE bands of **6** (0.98 eV) is in accord with the *6-syn* geometry and compares well with the calculated band separation of 1.26 eV for **6-syn**.

For the investigation of transannular interactions norbornadiene (**1**) represents a key compound²⁾. The two lowest radical cation states (2A_1 , 2B_2) of **1**, measured by photoelectron spectroscopy, differ from each other energetically by 0.85 eV³⁾. Ab initio calculations taking into account reorganization and correlation reproduce the experimental spectrum excellently and thus demonstrate the validity of Koopmans' theorem for **1** in the range of valence electrons⁴⁾. The theoretically deduced sequence of ion states or orbitals, resp., ($\tilde{X}^2B_2 < \tilde{A}^2A_1$, $b_2 > a_1$) could be verified experimentally by examining the longicyclically conjugated 7-isopropylidenenorbornadiene (**2**)⁵⁾. An important point in the argumentation has been that the necessarily b_2 -symmetrical isopropylidene π orbital of **2** (C_{2v}) only combines with the highest π orbital of the norbornadiene chromophore and therefore also determines the symmetry of the latter as b_2 . The C_{2v} symmetry of **2** also demands that $H_{ac} = H_{bc} \approx H_{ab}$ (cf. **3**) applies to the interaction matrix elements. However, this interpretation can no longer be employed for those norbornadienes, which possess a pyramidalized centre in position 7. Such bicyclic compounds include the 7-azanorbornadienes **4**. The unsymmetrical, hybridized nonbond-

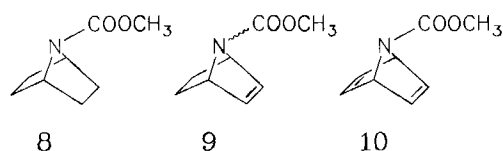
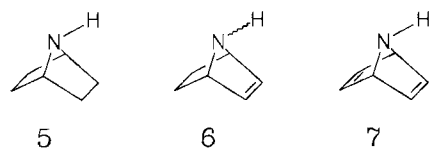
ing orbital n of the nitrogen atom need not necessarily show identical homoconjugative interaction parameters to the two localized orbitals π_a and π_b of norbornadiene, so that $H_{na} \neq H_{nb}$ will be generally true.

Such a dependence of the interaction of a hybridized nonbonding orbital on its orientation has often been discussed^{6–12)}. An additional problem qualitatively hardly to solve is the following: due to the reduced symmetry (C_s) in **4** compared to **2** the nonbonding orbital n in position 7 is allowed to mix strongly with the σ skeleton orbitals of the same symmetry. The corresponding mixing of the π orbital in position 7 in **2** is less intensive owing to the higher symmetry (C_{2v}) in **2**.

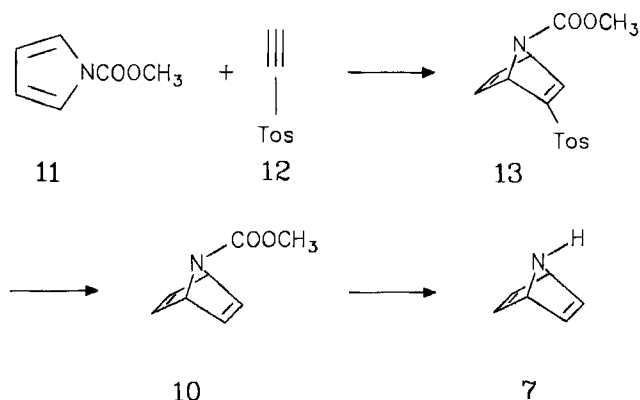
In this paper we report on the syntheses and photoelectron spectra of the 7-azabicyclic compounds **5**–**10**¹⁴⁾. A pro-



cedure suggested by Heilbronner and Schmelzer (abbreviated HS procedure) and the *ab initio* STO-3G model with a minimal basis set will be used for the interpretation of the spectra¹³.



thetic route allows to synthesize the compounds **7** and **10** easily in amounts of several grams from *N*-(methoxycarbonyl)pyrrole (**11**) as starting material.



Results

Syntheses

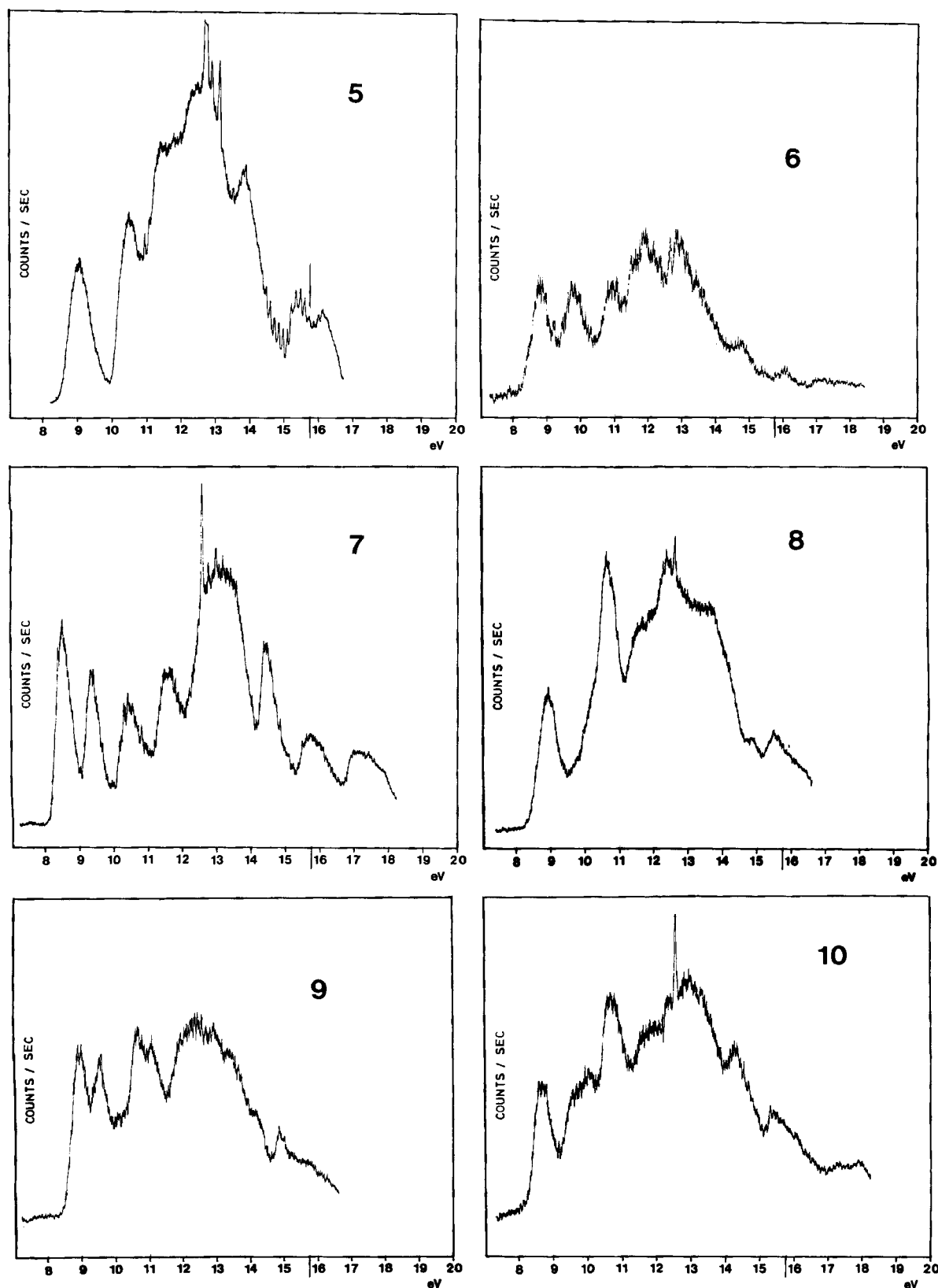
7-Azanorbornadiene (**7**) and its derivatives such as **10** have long defied preparation, since the back reaction mostly dominates in the obvious pathway by a Diels-Alder reaction of pyrrole derivatives with acetylenes. In those cases, in which a successful [4 + 2] cycloaddition can be achieved, the removal of the activating functional groups of diene and dienophile has given rise to serious problems¹⁴. Only by using the novel dienophilic acetylene equivalents¹⁵ ethynyl *p*-tolyl sulfone (**12**) Altenbach and Vogel made **7** accessible via **10** by a Diels-Alder route in 1982¹⁶. In addition to the simple reductive removal of the *p*-tolylsulfonyl group the key to success lay in the mild hydrolysis of the *N*-methoxycarbonyl function with trimethylsilyl iodide. The short syn-

A five-step synthesis of 7-azanorbornene (**6**)¹⁷ has already been known for some time. The double bond is thus introduced by an oxidative decarboxylation of a dicarboxylic acid, but this procedure did not turn out to be suitable for the preparation of **6** in sufficient amounts. After first attempts to synthesize the 7-azanorbornenes **6** and **9** in analogy to the preparation of **7** and **10** by a reaction of **11** with (*p*-tolylsulfonyl)ethylene failed, owing to the even higher tendency of azanorbornene derivatives to undergo a retro-Diels-Alder reaction¹⁸, a special synthetic route starting from **13** was developed for such systems.

Key step in this route is the selective catalytic hydrogenation of **13** with one equivalent of hydrogen and Pd/C as a catalyst to yield **14**. The desulfonation of **14** as well as the cleavage of the carbamate function of **9** can be carried out

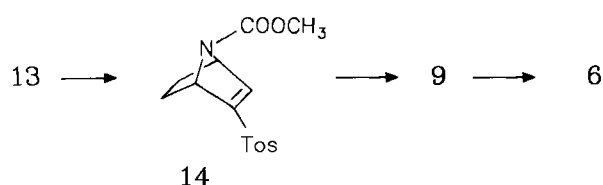
Table 1. Vertical ionization energies $I_{m,j}$ (eV) of compounds **5**–**10** and values calculated with Koopmans' theorem. If two different values are given, as for **6** and **9**, the first one refers to the invertomer in which N–R is oriented *syn* to the double bond and the second one to the structure in which N–R is orientated *anti* to the double bond (R = H, COOCH₃). The value in parentheses is uncertain, since the corresponding maximum could not be exactly evaluated due to overlapping bands

Compound	$I_{m,exp}$	MNDO	MINDO/3	HAM/3	STO-3G
5	$I_{m,1}$ 9.00	10.30	8.77	8.97	7.96
6	$I_{m,1}$ 8.75	9.85 9.73	8.54 8.74	9.04 8.93	7.51 7.71
	$I_{m,2}$ 9.73	10.63 10.39	9.56 9.40	9.73 9.62	8.77 8.25
7	$I_{m,1}$ 8.60	9.62	8.45	9.10	6.77
	$I_{m,2}$ 9.40	9.91	9.26	9.44	7.26
	$I_{m,3}$ 10.50	10.80	9.62	10.31	9.59
8	$I_{m,1}$ 8.93	10.12	9.11	8.95	
	$I_{m,2}$ 10.62	11.25	10.16	9.27	
		11.58	10.58	10.20	
9	$I_{m,1}$ 9.00	10.12 10.07	9.03 9.13	9.00 8.93	
	$I_{m,2}$ 9.60	10.51 10.48	9.49 9.48	9.39 9.32	
	$I_{m,3}$ 10.7	11.44 11.50	10.49 10.49	9.63 9.46	
		11.65 11.69	10.64 10.60	10.18 10.14	
10	$I_{m,1}$ 8.65	9.79	8.91	8.93	8.89
	$I_{m,2}$ (9.8)	10.25	9.31	9.45	9.34
	$I_{m,3}$ 10.03	10.46	9.72	9.52	9.61
	$I_{m,4}$ 10.70	11.37	10.50	9.76	9.69
		11.59	10.79	10.25	10.43

Figure 1. He(I α) Photoelectron spectra of 5–10

under such mild reaction conditions that no [4 + 2] cycloreversion takes place, and both **9** and **6** are obtained in pure form.

The completely saturated system **5** has long been known¹⁹, but may also be easily prepared by hydrogenation of **7**. Urethane **8** is accessible by hydrogenation of **10**.



Photoelectron Spectra

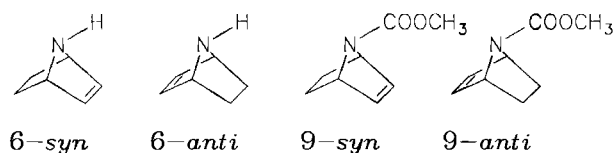
The $\text{He(I}_{\alpha})$ photoelectron spectra of **5**–**10** are depicted in Figure 1.

In Table 1 the ionization energies (eV) are given. They refer to the band maximum I_{mj} with an accurateness of ± 0.03 eV. The calibration is carried out with Xe (12.13, 13.44 eV) and Ar (15.76, 15.94 eV).

The results of semiempirical²⁰⁾ and ab initio²¹⁾ calculations, which allow an assignment of bands using Koopmans' approximation, are given in Table 1 as well.

Geometry Optimization and Structure

The geometry optimizations for all compounds **5**–**10** were carried out with the MNDO method, additionally for compound **6** with the ab initio STO-3-21G model and for **5**–**7** with the MM2 force field. Whereas for reasons of symmetry only one invertomer of the bicyclic compounds **5**, **7**, **8**, and **10** is calculated, a *syn*- or *anti*-invertomer is obtained in the case of **6** and **9** in which the ligand at the nitrogen atom is either orientated towards (*syn*) or away from (*anti*) the double bond.



Both MNDO and ab initio calculations for **6** result in a more stable *syn*-invertomer **6-syn** of azanorbornene: STO-

3-21G $\Delta E = 2.5 \text{ kcal} \cdot \text{mol}^{-1}$, MNDO $\Delta E = 0.6 \text{ kcal} \cdot \text{mol}^{-1}$. These results are in good agreement with ground state energies obtained by the 3G basis set.

Carrupt and Vogel²²⁾ calculated a stabilization of the *syn*-isomer of **6** by $1.24 \text{ kcal} \cdot \text{mol}^{-1}$. Energies calculated with the MM2 force field²³⁾ tend towards similar quantities: ΔH_f° (kcal \cdot mol $^{-1}$) for **6-syn** 10.87, **6-anti** 15.12. According to our knowledge the inversion barrier **6-syn** \rightarrow **6-anti** has not yet been determined experimentally. The calculated value of $12.5 \text{ kcal} \cdot \text{mol}^{-1}$ (MNDO) is of comparatively similar order as the measured and calculated inversion barrier of 7-methyl-7-azabicyclo[2.2.1]heptane (ΔH^\ddagger [kcal \cdot mol $^{-1}$]; NMR 15.3, AM1 10.0)²⁴⁾.

MNDO and MINDO/3 procedures were used for the urethanes **8**–**10**. The most important differences between the two optimization methods concern the pyramidalization angle carbonyl C atom/nitrogen atom/dummy: $\alpha(\text{C}-\text{N}-\text{D})$. The dummy is situated in the middle of the line connecting the two bridgehead carbon atoms. Whereas MINDO/3 calculations yield an almost planar nitrogen atom with an angle $\alpha(\text{C}-\text{N}-\text{D}) \approx 180^\circ$ (the exact value for **9** amounts to 174° , in which case the small *syn*- or *anti*-orientation of the ester group does not influence the enthalpy value), a clearly pyramidalized nitrogen atom is obtained by the MNDO method: $\alpha(\text{C}-\text{N}-\text{D}) = 164^\circ$ for **8**, 149° for **9-syn**, 146° for **10**. The **9-syn** isomer is more stable than **9-anti** [$\alpha(\text{C}-\text{N}-\text{D}) = 152^\circ$] by $0.5 \text{ kcal} \cdot \text{mol}^{-1}$. The AM1 method²⁵⁾, too, yields a pyramidalized geometry for **10** ($\alpha = 137^\circ$).

An interesting question is whether the PE spectrum of **6** can give any indication for the existence of two invertomers **6-syn** or **6-anti**. According to the calculation method and basis set applied (see above) an equilibrium portion of approximately 80 to 99% is predicted for the favored *syn*-isomer. This means, that photoionization should chiefly register the more stable invertomer (it is unlikely that the photoionization cross-sections of the two isomers will significantly differ from each other). Thus, the maxima of the two

Table 2. Calculated energies, angles, and dipole moments of compounds **5**–**10**. D is a dummy in the middle of the connecting line between the bridgehead atoms

	5	6-syn	6-anti	7	8	9-syn	9-anti	10
	H_f (kcal \cdot mol $^{-1}$) or E_{tot} (a.u.), resp.				H_f (kcal \cdot mol $^{-1}$)			
MM2	-24.22	10.87	15.12	53.10	–	–	–	–
MNDO	1.59	36.9	37.5	74.7	-74.5	-40.2	-39.77	-2.8
3-21G	–	-285.25103	-285.24704	–	–	–	–	–
	α (H-N-D) (degree)				α (C-N-D) (degree)			
MM2	125.5	124.4	126.1	125.0	–	–	–	–
MNDO	124.5	123.7	124.7	124.0	163.7	149.2	152.2	145.8
3-21G	–	122.4	123.4	–	–	–	–	–
	dipole moment (Debye)				dipole moment (Debye)			
MM2	1.00	0.73	1.38	1.27	–	–	–	–
MNDO	1.37	1.44	1.48	1.54	2.58	2.69	2.75	2.75
3-21G	–	1.41	1.69	–	–	–	–	–

comparatively symmetrical bands can be ascribed to the **6-syn** isomer. However, it cannot be excluded, that the minor signals of low intensity to be discerned on the right hand flank result from **6-anti**, or that the less intensive signals of **6-anti** are hidden under the relatively broad basis of the two bands.

An additional indication for the prevailing existence of **6-syn** is given by the distance between the first two bands. On calculating the mean value from the calculated differences $\varepsilon_1 - \varepsilon_2$ (MNDO, MINDO/3, HAM/3, STO-3G) for each of the *syn*- and *anti*-isomer, $\Delta\varepsilon_{1,2}(\text{syn}) = 0.93$ eV and $\Delta\varepsilon_{1,2}(\text{anti}) = 0.63$ eV, it can be observed that within the limit of error $\Delta\varepsilon_{1,2}(\text{syn})$ practically corresponds with $\Delta I_{1,2}^m = 0.98$ eV.

Thus, in the following discussion the measured ionization energies of **6** will be interpreted by means of the *syn*-orientation. In Table 2 relevant structural data are summarized.

Discussion

Canonical Molecular Orbitals (CMO)

The results of various calculations are given in Table 1. It is known, that calculations with MINDO/3 and HAM/3 lead to useful predictions both for the *n* and π levels. Equally well-known is the fact that (within the scope of Koopmans' approximation) STO-3G ionization energies may be too low by about 1–2 eV, whereas according to the MNDO model ionization energies are calculated too high by ca. 1 eV^{2b)}. Since the orbital sequences of the tabulated levels of **5**, **6**, and **7** show no significant differences between the four methods, only the results of the *ab initio* STO-3G method will be explained more precisely. In Figure 2 are depicted the corresponding wave functions based on the localized bond orbitals (see further below). The following observations are remarkable:

a) In addition to the expected contribution of the CN bonds in **5** the high proportion of the *anti*-orientated 1,2- and 3,4-CC- σ bonds is particularly striking. Those σ bond orbitals mix into the lone pair of nitrogen in an antibonding way. This delocalization of the *n* orbital causes the comparatively low ionization energy of 9.0 eV.

b) Besides there is a further effect in **6-syn**: the direct interaction (homoconjugation) with the π orbital. However, the sequence and splitting of the two highest occupied levels is not only a consequence of the direct overlap of *n* and π , but is also essentially brought about by the σ bond orbitals involved.

c) The picture of **6-anti** differs from that. On the one hand the split between the two levels is smaller (0.54 eV for **6-anti** vs. 1.26 eV for **6-syn**), on the other hand direct homoconjugation appears to be less significant than for **6-syn**. In both levels the electron pair shows a *bonding* relationship to π .

d) For **7** a combination of the effects described in a)–c) is observed. It is conspicuous that the *n* character (or percentage of electron pair) increases from the highest level (6.77 eV) to the third highest (9.59 eV).

On examining the wave functions in Figure 2 two questions remain unanswered. On the one hand, the relative weight of both the direct interaction between *n* and π and the through-bond coupling via σ orbitals can not easily be inferred from the diagrams. On the other hand, the problem arises, whether the relative composition of that wave function of π and *n* portions can be examined experimentally. The first question will be dealt with further below within the scope of the HS procedure with localized orbitals. For the investigation of the *n* contribution to the wave function a He(II)-PE spectrum has been measured.

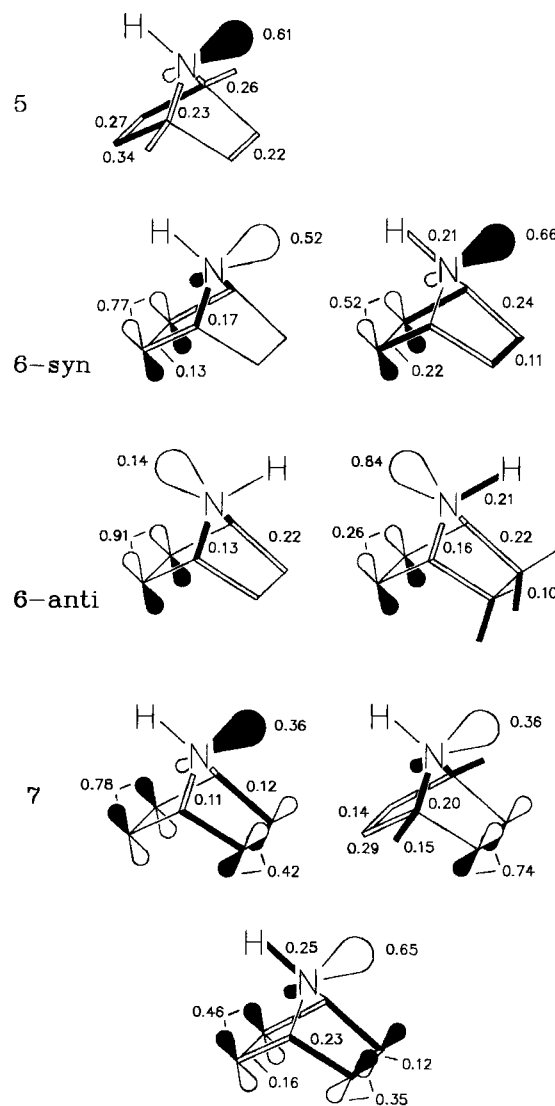


Figure 2. Canonical STO-3G wave functions (CMO) in the basis of the bond orbitals. Portions <0.1 have not been considered. In sequence and energy of the CMO correspond to those given in Table 1

He(II)-PE Spectrum of **7**

PE band intensities are theoretically described as photoionization cross-sections²⁶⁾. Schweig and Thiel have presented a theoretical model which allows to interpret the observed relative differences in intensities following the

change from He(I) to He(II) radiation²⁷⁾. The equation for the total photoionization cross-section is:

$$\sigma_n = A \cdot \beta_n \left[\sum_a Q_a + \sum_{a < b} Q_{ab} \right] / E_{ph}$$

It is assumed here that the measured differential cross-section $d\sigma(90^\circ)$ contains an asymmetry parameter β_n which does not alter when changing from He(I) to He(II) radiation. In the equation given above the photon energy E_{ph} as well as the one-centre terms Q_a are important for the case at hand. The photon energy amounts to $E_{ph}(\text{HeI}) = 21.22$ eV or $E_{ph}(\text{HeII}) = 40.81$ eV, resp. The one-centre terms depend on both the squares of the atomic orbital coefficients of the molecular orbital to be ionized and the square of the transition moment. Schweig and Thiel point out that the low energy He(I) photoelectrons show an optimal overlap with carbon 2p atomic orbitals, whereas He(II) photoelectrons of higher energy display good overlap with nitrogen, oxygen, and fluorine 2p atomic orbitals²⁷⁾. Thus, one-centre terms with large coefficients for nitrogen should increase in going from He(I) to He(II) radiation. In Table 3 the theoretical and experimental data for pyrrole as a good reference for azanorbornadiene (7) are contrasted with the experimental results (cf. Figure 3) of 7.

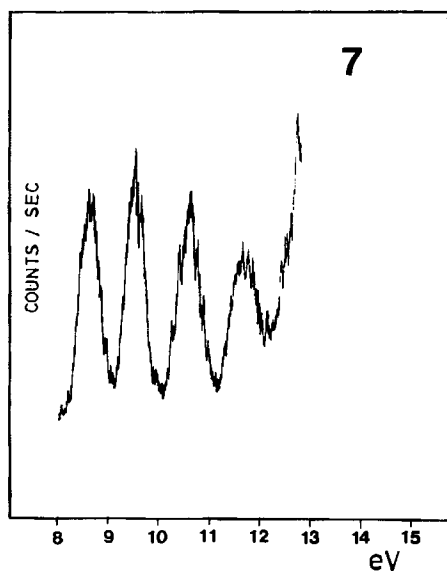


Figure 3. He(II) PE spectrum of 7

Table 3. Relative band intensities in He(I) and He(II) photoelectron spectra of pyrrole²⁷⁾ and azanorbornadiene (7)

Compound	I_m/eV	Relat. band intensity, exp. (theor.)	
		He(I)	He(II)
Pyrrole ²⁷⁾	8.21 (1a ₂)	100 (100)	100 (100)
	9.20 (2b ₁)	89 (72)	140 (100)
7	8.60 (a')	100	100
	9.40 (a')	79	103
	10.50 (a')	93	114

Just as an increase in intensity of the second band [$b_1(\pi)$ -MO, large coefficient for nitrogen] can be observed for pyrrole, an increase in intensity for the second and third band of 7 can also be noticed, which is in agreement with the information given in Figure 2.

Localized Molecular Orbitals (LMO)



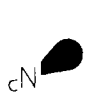


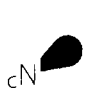
In order to deal with the problem of separating the direct interactions of π and n from the σ coupling (through bond) in the scope of a suitable model, the HS procedure is chosen¹³⁾. The following definition proved to be useful: A direct interaction (through space) between the localized orbitals π and n of 6 will be found if its matrix element $F_{\lambda,\pi n}$ in the Hartree-Fock matrix F_λ differs significantly from zero.

In that case is

$$F_\lambda = L \cdot F_\phi \cdot L^T \quad \text{and} \quad \lambda = L \cdot \phi$$

Here F_ϕ contains the basis of CMO ϕ (STO-3G) and F_λ the basis of LMO λ ; L is an orthogonal transformation matrix. The transformation matrix L is chosen according to the localization criterion by Foster and Boys, that means maximization of the sum of the squared distances between the charge centres of each molecular orbital²⁸⁾. The localized banana orbitals of the double bonds are then converted into common σ and π orbitals. The diagonal elements of F_λ , the basis energies $F_{\lambda,ii}$ ($i = \pi, n$) of the localized orbitals LMO and the interaction matrix elements $F_{\lambda,\pi n}$ for 6 and 7 are given in Table 4.

Table 4. HF matrix F_λ in the LMO basis. Only the *syn*- or *anti*- π orbitals (in relation to N-H) as well as the n electron pair are presented here. The values given in each box relate from top to bottom to 6-*syn*, 6-*anti* and 7. Energies are given in eV

	 syn-NH	 anti-NH	 cN
 syn-NH	-8.76 -8.34	— -0.96	0.66 0.90
 anti-NH	— -0.96	— -8.54 -8.34	— -0.74 -0.42
 cN	0.66 — 0.90	— -0.74 -0.42	-13.61 -13.58 -14.06

It should be noted, that the direct interaction evidently depends on the orientation of the electron pair of nitrogen. Furthermore, it should be stated that the terms $F_{\lambda,\pi n}^{syn}$ of 6-

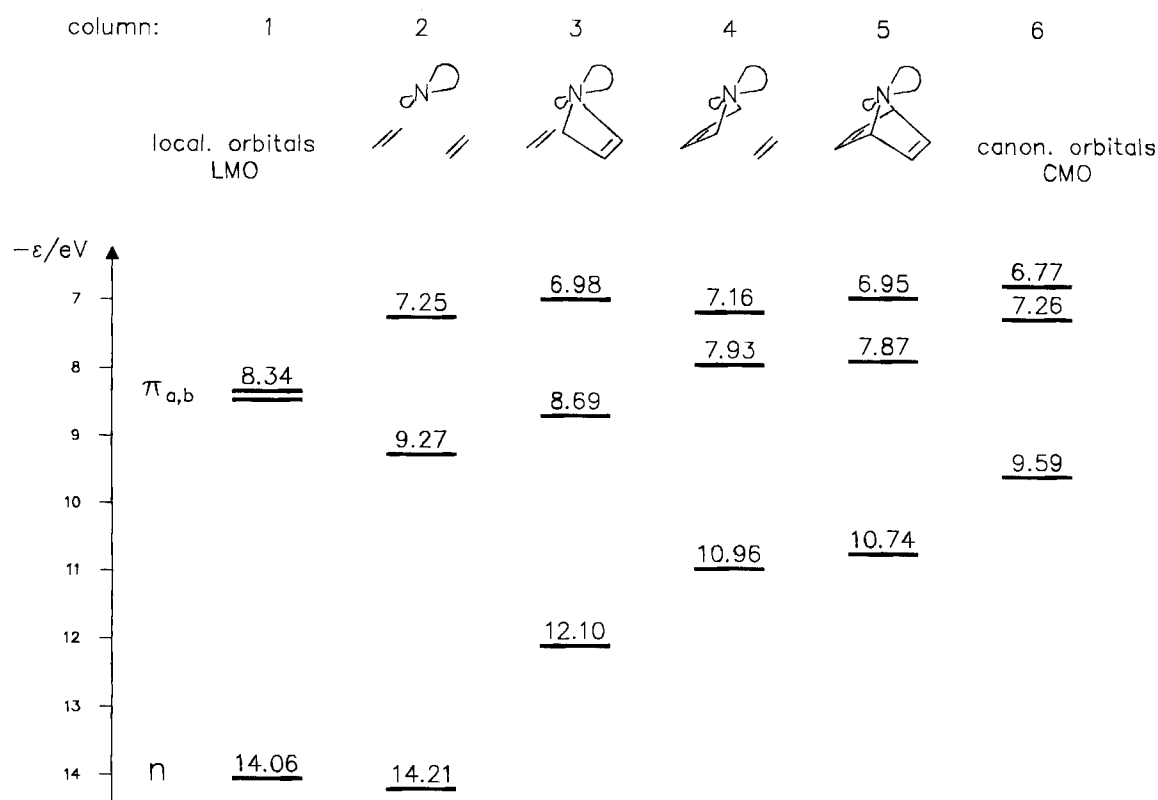


Figure 4. Stepwise construction of STO-3G CMO of **7** in the basis of the localized bond orbitals LMO (cf. Figure 2). The construction starts with the LMO in column 1 and finally leads to the CMO of **7** via the through-space interaction (column 2) and inclusion of different fragment orbitals (columns 3–5)

syn and **7** are not identical; the same applies to $F_{\lambda,\pi n}^{anti}$. This is due to slight differences in geometry (e.g. angle of inclination of the CNC bridge towards the double bond etc.). According to the definition of the direct (through-space) interaction given above it can be said that **n** and π_i ($i = syn, anti$ or *a, b*, resp.) of **6** and **7** as well as π_a and π_b of **7** of course show a considerable homoconjugation (through-space interaction). For a comparison of the quantities the interaction term $F_{\lambda,\pi a \pi b}$ of the two π orbitals of norbornadiene (**1**) according to a MINDO/2 calculation is $F_{\lambda,\pi a \pi b} = -0.78 \text{ eV}^{13a}$.

On the other hand this homoconjugation between π_a , π_b , and **n** is not capable of reproducing even approximately the orbital sequence, which is obtained by a complete canonical calculation. This can immediately be realized by comparing the columns 1 (LMO), 2 (through-space interaction of LMO), and 6 (sequence of the CMO's according to Table 1) of Figure 4 with each other.

Thus, the consideration of relevant σ orbitals is indispensable.

Construction of Fragment Orbitals

In columns 3 and 4 of Figure 4 the **n** electron pair is extended, that means relevant σ orbitals of the LMO basis are added and combined with $\pi_{a,b}$ and **n**; on the whole 8 LMOs are used in columns 3 and 4. The result in column 4 is more similar to the scheme aimed at in column 6 than

the sequence in column 3. The reason for that lies at hand: the selection of relevant σ LMOs turns out to be better in column 4. For a fairly adequate description of the lone pair of **7** the two C–N and the two 1,2- and 3,4-CC σ bonds are obviously essential, that means the σ bonds on the back of the **n** electron pair (anti-orientated σ bonds) are more relevant in this case than those on the front side. Column 5 integrates the **n** electron pair completely into the skeleton σ orbitals, however, the effect compared to column 4 is negligible, which emphasizes again the importance of the anti-orientated 1,2- and 3,4-CC σ orbitals.

In the empirical PE spectroscopy experimental ionization energies of reference compounds are often used as basis energies for orbital interactions. Applying this to the case at hand would mean that the **n** ionization energy of 7-azanorbornane (**5**) is interpreted as the “**n** electron pair basis energy” of **7**. That this is only permissible, if the delocalized character of the electron pair is taken into account, follows directly from Figures 4 and 5. The basis energy of the “pure” electron pair amounts to ca. -14 eV (Figure 4, column 1), however, the measured ionization energy is $I_{m,1} = -9.0 \text{ eV}$. Figure 5 demonstrates which σ LMOs are necessary to rise the basis energy $F_{\lambda,nn} \approx -14 \text{ eV}$ to the level of the experimentally measured orbital energy $\epsilon_{\text{exp}}(\mathbf{5}) = -9.0 \text{ eV}$.

Apart from the C–H LMO of the ethano bridges all other σ LMOs are combined with **n**. This results in a fragment orbital **n**_{frag} whose energy $\epsilon_{\text{frag}} = -9.11 \text{ eV}$ is surprisingly close to the experimental value of **5** (Figure 5, column

1); the geometry of **6-anti** is taken here. In column 2 the same procedure is repeated for the geometry of **6-syn**; the fragment orbital energy obtained is practically unchanged $\epsilon_{\text{frag}} = -9.19$ eV. It should be stressed that the destabilizing effect of the σ system from $F_{\lambda,nn} \approx -14$ eV to $\epsilon_{\text{frag}} = -9.11$ eV calculated by STO-3G is reflected in the following experimental difference: ionization energy of atomic nitrogen 14.55 eV²⁹, ionization energy of azanorbornane (**5**) 9.0 eV.

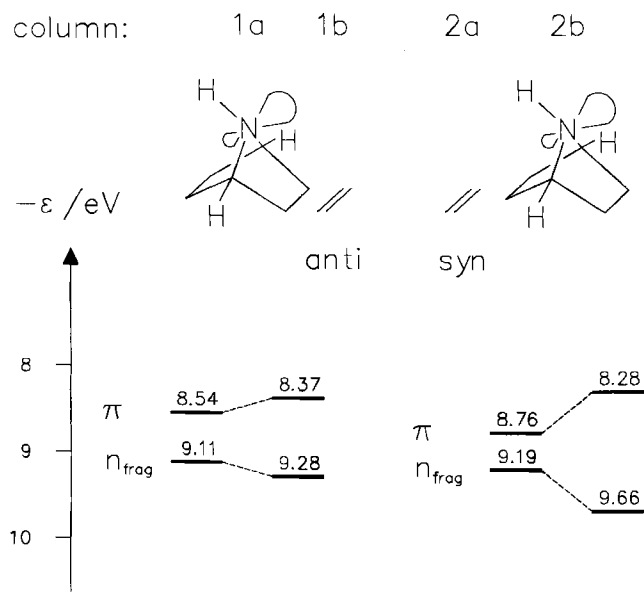


Figure 5. Construction of a fragment orbital n_{frag} from n and 11 σ -LMO. Column 1a: **6-anti** geometry; Column 2a: **6-syn** geometry; Column 1b: interaction of n_{frag} with π_{anti} ; Column 2b: interaction of n_{frag} with π_{syn}

Furthermore, the effect of an interaction between the fragment orbital n_{frag} and π is interesting. Depending on the *syn*- or *anti*-orientation of π in relation to N–H a larger (Figure 5, column 2) or smaller (column 1) split is obtained. Just this is also shown by detailed calculations of canonical wave functions (Table 1).

Precanonical Molecular Orbitals (PCMO)

In the preceding passage the importance of the σ system (pictured as localized σ bond orbitals) for the energy and sterical, orientated interaction of the n electron pair has been demonstrated. In a last step it will now be shown, which completely delocalized σ orbitals combine to which extent with the electron pair n . In order to obtain those PCMO Ψ , new symmetry-adapted, semi-localized molecular orbitals are created from the LMOs and used as a basis for the HF Matrix F_Q^{13a} . In the submatrix of $F_Q(A')$ belonging to the irreducible representation A' all off-diagonal elements in the column and row of the n electron pair are eliminated. The diagonalization then yields the precanonical energies, the PCMOs $\Psi(A')$ and the transformation matrix $P_n(A')$. Finally, the application of $P_n(A')$ to $F_Q(A')$ leads to the matrix $F_\Psi(A')$, which links the PCMO $\Psi(A')$ with the electron pair n .

Table 5. HF matrix $F_\Psi(A')$ of PCMOs of the compounds **6-syn**, **6-anti**, and **7**, which interact with the electron pair n at the nitrogen atom. Energies are given in eV. Only the energetically highest PCMOs are listed here

	-7.98	0	0	0	-0.71	0
	0	-11.82	0	0	-0.05	0
	0	0	-12.62	0	1.37	0
	0	0	0	-12.78	-1.39	0
	-0.71	-0.05	1.37	-1.39	-13.61	1.31
	0	0	0	0	1.31	-14.98

	-7.72	0	0	-0.09	0	0
	0	-11.90	0	-0.66	0	0
	0	0	-12.15	-0.58	0	0
	-0.09	-0.66	-0.58	-13.58	1.62	2.54
	0	0	0	1.62	-14.00	0
	0	0	0	2.54	0	-14.70

	-6.94	0	0	0	-0.48	0
	0	-7.84	0	0	-0.89	0
	0	0	-10.98	0	-0.46	0
	0	0	0	-12.87	1.87	0
	-0.48	-0.89	-0.46	1.87	-14.22	0.42
	0	0	0	0	0.42	-14.43
	0	0	0	0	-2.08	0
	0	0	0	0	-2.08	-15.48

The only off-diagonal matrix elements of $F_\Psi(A')$ are those, which indicate the interaction with the electron pair n . In Table 5 those matrices $F_\Psi(A')$ are given for **6-syn**, **6-anti**, and **7**.

It has now become possible to make important statements concerning the role played by the electron pair in relation to the π and σ orbitals.

7-Azanorbornene (6-syn)

a) The electron pair shows high off-diagonal matrix elements for those σ PCMOs which have larger contributions in the CN bonds and the CC bonds at the back. This result is in agreement with that shown in Figure 4 (column 4). Thus, a good representation of the electron pair of all four compounds **5**, **6-syn**, **6-anti**, and **7** is the highest CMO of **5** depicted in Figure 2.

b) The interaction with the π PCMO is considerable: $F_{\Psi, n\pi}^{\text{syn}} = -0.70$ eV. Hereby the sterically favored electron pair interaction at the back also becomes evident.

7-Azanorbornene (6-anti)

a) The contributions of the σ PCMOs are similar to those of **6-syn**.

b) However, the most remarkable difference to **6-syn** concerns the matrix element $F_{\Psi, n\pi}^{\text{anti}} = -0.09$ eV. Naturally, it cannot be concluded that the direct homoconjugation is negligible. With regard to Table 4 ($F_{\lambda, \pi n} = -0.74$ eV) exactly the opposite is more convincing. On the contrary, the all but simple parameter $F_{\Psi, n\pi}^{\text{anti}} = -0.09$ eV is the consequence of combined through-space and through-bond interactions which almost compensate each other. This is also shown by the fact that the precanonical orbital energy $\varepsilon_{\text{PCMO}} = -7.72$ eV from Table 5 (middle part) is practically identical to the canonical orbital energy from Table 1, $\varepsilon_{\text{CMO}} = -7.71$ eV. It should be recorded: *due to contrary, compensatory effects, n and the π PCMOs of 6-anti finally hardly combine with each other any more.*

7-Azanorbornadiene (7)

a) Just as for **6** the contributions of the σ PCMOs are important and sterically analogous.

b) The indication for differences in the comparison of **7** with isopropylidenenorbornadiene (**2**) given in the introduction can now be specified. Owing to its C_{2v} symmetry the isopropylidene π Orbital of **2** can clearly differentiate between the orbitals $\pi(b_2)$ and $\pi(a_1)$. The electron pair **n** of **7**, however, combines with both π combinations but the interactions term with the symmetrical combination turns out to be larger: $F_{\Psi, n\pi+} = -0.89$ eV, $F_{\Psi, n\pi-} = -0.48$ eV.

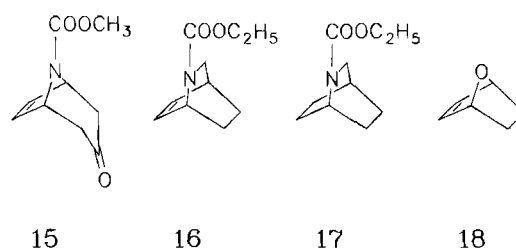
Summary of the Results for **5**, **6**, and **7**

Besides the CN bonds the three CC bonds sterically orientated towards the back are essential in the description of the electron pair. The interaction of the "pure" electron pair (LMO) with the σ -coupled π orbitals (PCMO) depends on the orientation: in **6-syn** considerable, in **6-anti** only insignificant interactions are observed. However, in **7** **n** combines with both π molecular orbitals, since in that molecule those π PCMOs appear as linear combinations of the two localized orbitals π_a and π_b . It is interesting, that the invertomer which has a higher ground state stability and therefore has

been measured PE spectroscopically (**6-syn**) should also yield a larger π -**n** split according to theoretical predictions (1.26 eV, STO-3G). This is supported by the observed split of 0.98 eV.

Urethanes

Although unsaturated bicyclic urethanes have been investigated PE-spectroscopically no indications for direct or indirect proximity effects have so far been obtained^{30,31}. Neither for **15** nor for **16** a direct homoconjugation could be revealed spectroscopically (though no symmetry restriction would exclude a π - π interaction). Only the inductive stabilization of the π_{CC} orbital of **15** by the electronegative urethane function (group electronegativity 2.62) has been observed and identified as such by inspection of the π_{CC}^* orbital³¹.



Due to the structural similarity of **9** to **15** one would also expect the existence of essentially isolated chromophores in the former norbornene derivative. Since all SCF methods allow only incomplete statements concerning the PE spectra of **8**–**10**, the empirical interpretation by means of the reference compounds **15**–**17** is to be preferred.

The urethane group displays three characteristic valence orbitals which are ionized in the range of 8–11 eV. Urethane **17** may serve as an example³⁰: $I_{m,1} = 8.43$ eV (n_N , chiefly localized at the nitrogen atom), $I_{m,2} = 9.67$ eV (n_O , typical electron pair of a carbonyl oxygen atom), and $I_{m,3} = 10.50$ eV (π_{OO} , typical π MO of the ester group with contributions of both oxygen atoms).

For urethane **8** n_N can exactly be identified ($I_{m,1} = 8.93$ eV), whereas n_O and π_{OO} are to be found in the second, extremely broad PE band with a maximum at 10.62 eV.

The unsaturated urethane **9** shows two ionisation events at 9.00 and 9.60 eV, of which the first one is ascribed to the n_N level and the second one to the π_{CC} orbital. Since the urethane function roughly has the same inductive effect as the ether oxygen atom of **18**³¹ ($\delta\alpha \approx -0.6$ eV), this assignment is relatively reliable (cf. the position of the π_{CC} orbital of **18** at 9.44 eV³²). Thus, the ionizations of the urethane-specific levels n_O and π_{OO} are to be located at 10.7 eV, which is in good agreement with the measured values of **8**.

The expected five valence orbitals of the most interesting compound **10** can, partly exactly, partly approximately, be inferred from the spectrum. As for **8** and **9**, n_O and π_{OO} is found in the intensive band at 10.70 eV. Thus, the ionization at 8.65 eV (one level) and the broad band at 10.0 eV (with an obvious shoulder at ca. 9.8 eV) is left for the remaining three levels. These refer to combinations of the three valence

orbitals n_N , π_+ , and π_- . The following two observations are in favour of an evident homoconjugation between n_N and π_- :

- The destabilized position of the highest level at 8.65 eV.
- The characteristic splitting pattern 1:2, which amazingly reminds of isopropylidenenorbornadiene (**2**) or methylenenorbornadiene (8.50, 9.65, 9.90 eV)⁵.

However, the degree of pyramidalization of the nitrogen atom remains uncertain. With a *local* C_{2v} symmetry (planar structure at the nitrogen atom) facts would be analogous to **2**. With a *local* C_s symmetry (pyramidal structure) combinations analogous to **7** would exist. In both cases the homoconjugation between π_- (and possibly also π_+) and n_N has a destabilizing effect on the first valence orbital, which is in agreement to the experimental result.

The fact that homoconjugation is observed for **10** but not for **9** or **15** and **16**, resp., may be rationalized by a simple reason: due to electron-electron repulsion in **9**, **15**, and **16** the functional groups can withdraw themselves from each other, so that a significant overlap no longer takes place. In **10**, however, this is impossible. If the urethane bridge tries to avoid the left double bond π_a it will inevitably come close to π_b and vice versa. For **10** the conformation of minimal energy will necessarily show the phenomenon of homoconjugation (and, of course, through-bond interactions which have been discussed in detail for **7**).

We appreciate financial support by the *Deutsche Forschungsgemeinschaft*, the *Fonds der Chemischen Industrie*, and the *BASF AG*.

Experimental

PE: Leybold-Heraeus Spectrometer UPG 200. — NMR: Bruker WM 300, Bruker HX 90. — MS: Finnigan MAT HSQ 30.

For the synthesis of 7-azabicyclo[2.2.1]hepta-2,5-diene (**7**) see ref.¹⁶.

7-(Methoxycarbonyl)-2-(*p*-tolylsulfonyl)-7-azabicyclo[2.2.1]hept-2-ene (**14**): To 2.0 g (6.5 mmol) of 7-(methoxycarbonyl)-2-(*p*-tolylsulfonyl)-7-azabicyclo[2.2.1]hepta-2,5-diene (**13**)¹⁶ in 15 ml of acetonitrile was added 1 g of Pd/C. The reaction vessel was rendered inert and afterwards purged with hydrogen. 225 ml (10 mmol) of hydrogen was led into the reaction mixture with rigorous stirring at room temperature. Finally, the catalyst was removed by filtration over Celite®, and the solvent was evaporated in vacuo. The remaining solid was recrystallized from ether/pentane adding some activated charcoal: 1.94 g (95%) of **14**, m.p. 115°C (ether/pentane). — ¹H NMR (90 MHz, CDCl₃): δ = 1.2–1.4 (m, 2H), 1.9–2.15 (m, 2H), 2.41 (s, 3H), 3.55 (s, 3H), 4.90 (m, 2H), 7.05 (m, 1H), 7.43 and 7.90 (m, 4H).

$C_{15}H_{17}NO_4S$ (307.4) Calcd. C 58.62 H 5.58
Found C 58.41 H 5.49

7-(Methoxycarbonyl)-7-azabicyclo[2.2.1]hept-2-ene (**9**): 3.1 g (10 mmol) of **14** was dissolved in 40 ml of dried THF and 20 ml of dried methanol under argon. After addition of 5.7 g (40 mmol) of anhydrous disodium hydrogenphosphate and 5.4 g (30 mmol) of sodium dihydrogenphosphate the reaction mixture was cooled to –78°C. In the course of 1 h 5.5 g (25 mmol) of 6% sodium amalgam was added in several portions with vigorous stirring. Then the solution was allowed to warm up, and the solvent was decanted from the solid residue, which was extracted once with 10 ml of ether and twice with pentane. The organic layers were combined, con-

centrated and filtered over aluminium oxide (activity II–III, 0.063–0.200 mm), adding ether/pentane (1:1) as a solvent. The solvent was then removed and the crude product purified by CC (silica gel 0.05–0.2 mm; column 25 × 1.6 cm; ether/pentane 1:1). The first fraction containing the product was concentrated and distilled in high vacuum: 0.42 g (37%) of **9**, b.p. 34°C/6 × 10^{–4} mbar. — ¹H NMR (90 MHz, CDCl₃): δ = 1.1–1.3 (m, 2H), 1.75–1.95 (m, 2H), 3.65 (s, 3H), 4.75 (m, 2H), 6.25 (s, 2H). — ¹³C NMR (CDCl₃): δ = 23.1, 24.1, 53.0, 59.2, 134.0, 134.9, 156.0.

$C_8H_{11}NO_2$ (153.2) Calcd. C 62.73 H 7.24
Found C 62.59 H 7.03

7-Azabicyclo[2.2.1]hept-2-ene (**6**): To 400 mg (2.6 mmol) of **9** in 10 ml of chloroform and 3 ml of a 0.8 M solution of trimethylamine in chloroform was slowly added 0.63 ml (3.2 mmol) of iodotrimethylsilane at –78°C. The reaction mixture was allowed to warm up and was then refluxed for 3.5 h. Then 1.0 g (17 mmol) of trimethylamine in 10 ml of chloroform was added to bind excess iodotrimethylsilane. The mixture was filtered under argon, the residue washed three times with 10-ml portions of chloroform, and the solvent removed in vacuo. To the remaining crude, hydrolysis-sensitive 7-[(trimethylsiloxy)carbonyl]-7-azabicyclo[2.2.1]hept-2-ene was added 5 ml of dichloromethane. To this solution was slowly dropped 0.1 ml (2.4 mmol) of dried methanol under argon at room temp. The initially foaming reaction mixture was heated to reflux for 10 min, and afterwards the solvent was removed at 65 mbar/room temp. The residue was purified by vacuum distillation. 180 mg (73%) of **6**, b.p. 36°C/26 mbar. — ¹H NMR (300 MHz, CDCl₃): δ = 1.01 (m, 2H), 1.72 (m, 2H), 1.97 (s, 1H), 4.09 (m, 2H), 6.19 (m, 2H). — ¹³C NMR (CDCl₃): δ = 24.6, 58.7, 60.8, 137.0.

$C_6H_{10}N$ Calcd. 96.0813 Found 96.0802 (MS)

7-(Methoxycarbonyl)-7-azabicyclo[2.2.1]heptane (**8**): To 1.0 g (6.5 mmol) of **10** in 10 ml of dried acetonitrile was added 0.5 g of Pd/C catalyst. The reaction vessel was rendered inert and purged with hydrogen for a short time. Under vigorous stirring 146 ml (6.5 mmol) of hydrogen was led into the reaction mixture. Then the catalyst was removed by filtration over Celite® and the solvent was removed in vacuo. The yellow, oily residue was purified by distillation in high vacuum. 0.92 g (90%) of **8**, b.p. 35°C/8 × 10^{–5} mbar. — ¹H NMR (90 MHz, CDCl₃): δ = 1.21–1.8 (m, 8H), 3.62 (s, 3H), 4.50 (m, 2H).

$C_8H_{13}NO_2$ (155.2) Calcd. C 61.91 H 8.44
Found C 61.78 H 8.32

7-Azabicyclo[2.2.1]heptane (**5**): To 275 mg (3.0 mmol) of **7**¹⁶ in 4 ml of dried methanol was added 137 mg of a 5% Pd/CaCO₃ catalyst. Under vigorous stirring **7** was hydrogenated with 134 ml of hydrogen. Then the reaction mixture was filtered over Celite®, and at 65 mbar the filtrate was concentrated carefully by means of a dry ice-cooled trap. The remaining residue was purified by vacuum distillation. 207 mg (70%) of **5**, b.p. 29°C/26 mbar, m.p. of picrate 183°C (ref.¹⁹) 171–173°C).

CAS Registry Numbers

5 - picrate: 27514-09-6 / **7**: 7092-27-5 / **8**: 131179-08-3 / **9** (syn): 131179-09-4 / **9** (anti): 131179-10-7 / **10**: 83060-75-7 / **13**: 83060-74-6 / **14**: 131193-46-9 / 7-azanorbornane: 279-40-3 / 7-azanorbornene: 55590-24-4

¹⁾ Dedicated to Professor *Edgar Heilbronner* on the occasion of his 70th birthday.
Part 73: K. Hassenrück, H.-D. Martin, R. Walsh, *Chem. Rev.* **89** (1989) 1125.

- 2) ^{2a)} H. D. Martin, B. Mayer, *Angew. Chem.* **95** (1983) 281; *Angew. Chem. Int. Ed. Engl.* **22** (1983) 283. — ^{2b)} H. D. Martin, B. Mayer, R. W. Hoffmann, A. Riemann, P. Rademacher, *Chem. Ber.* **118** (1985) 2514.
- ³⁾ P. Bischof, J. A. Hashmall, E. Heilbronner, V. Hornung, *Helv. Chim. Acta* **52** (1969) 1745.
- ⁴⁾ W. v. Niessen, G. H. F. Diercksen, *J. Electron Spectrosc. Relat. Phenom.* **16** (1979) 351.
- ⁵⁾ E. Heilbronner, H. D. Martin, *Helv. Chim. Acta* **55** (1972) 1490.
- ⁶⁾ G. R. Underwood, H. S. Friedman, *J. Am. Chem. Soc.* **99** (1977) 27.
- ⁷⁾ I. Morishima, K. Yoshikawa, M. Hashimoto, K. Bekki, *J. Am. Chem. Soc.* **97** (1975) 4283.
- ⁸⁾ J. B. Grutzner, *J. Am. Chem. Soc.* **98** (1976) 6385.
- ⁹⁾ H. Schmidt, A. Schweig, A. G. Anastassiou, H. Yamamoto, *J. Chem. Soc., Chem. Commun.* **1974**, 218.
- ¹⁰⁾ K. Yoshikawa, A. Matsui, I. Morishima, *J. Chem. Soc., Perkin Trans. 2*, **1977**, 1057.
- ¹¹⁾ K. Yoshikawa, K. Bekki, M. Karatsu, K. Toyoda, T. Kamio, I. Morishima, *J. Am. Chem. Soc.* **98** (1976) 3272.
- ¹²⁾ I. Morishima, K. Yoshikawa, *J. Am. Chem. Soc.* **97** (1975) 2950.
- ¹³⁾ ^{13a)} E. Heilbronner, A. Schmelzer, *Helv. Chim. Acta* **58** (1975) 936. — ^{13b)} G. Bieri, J. D. Dill, E. Heilbronner, A. Schmelzer, *Helv. Chim. Acta* **60** (1977) 2234.
- ¹⁴⁾ Cf. efforts by H. Prinzbach, H. Babsch, *Heterocycles* **11** (1978) 113; H. Prinzbach, H. Bingmann, H. Fritz, J. Markert, L. Knothe, W. Eberbach, J. Brokatky-Geiger, J. C. Sekutowski, C. Krüger, *Chem. Ber.* **119** (1986) 618.
- ¹⁵⁾ Review: O. De Lucchi, L. Pasquato, *Tetrahedron* **44** (1988) 6755.
- ¹⁶⁾ H.-J. Altenbach, B. Blech, J. A. Marco, E. Vogel, *Angew. Chem. Int. Ed. Engl.* **21** (1982) 789; *Angew. Chem. Suppl.* **1982**, 1614; *Angew. Chem. Int. Ed. Engl.* **21** (1982) 772.
- ¹⁷⁾ A. P. Marchand, R. W. Allen, *J. Org. Chem.* **40** (1975) 2551.
- ¹⁸⁾ L. J. Kricka, J. M. Vernon, *Adv. Heterocycl. Chem.* **16** (1974) 87.
- ¹⁹⁾ R. R. Fraser, R. B. Swingle, *Can. J. Chem.* **48** (1970) 2065.
- ²⁰⁾ ^{20a)} M. J. S. Dewar, W. Thiel, *J. Am. Chem. Soc.* **99** (1977) 4899. — ^{20b)} R. C. Bingham, M. J. S. Dewar, D. H. Lo, *J. Am. Chem. Soc.* **97** (1975) 1285. — ^{20c)} L. Asbrink, C. F. Fridh, E. Lindholm, *Chem. Phys. Lett.* **52** (1977) 69.
- ²¹⁾ W. J. Hehre, R. F. Stewart, J. A. People, *J. Chem. Phys.* **51** (1969) 2657.
- ²²⁾ P. Carrupt, P. Vogel, *J. Mol. Struct. (Theochem.)* **124** (1985) 9.
- ²³⁾ S. Profeta, N. L. Allinger, *J. Am. Chem. Soc.* **107** (1985) 1907.
- ²⁴⁾ S. F. Nelsen, J. T. Ippoliti, T. B. Frigo, P. A. Petillo, *J. Am. Chem. Soc.* **111** (1989) 1776.
- ²⁵⁾ M. J. S. Dewar, E. G. Zoebisch, E. F. Healy, J. J. P. Stewart, *J. Am. Chem. Soc.* **107** (1985) 3902.
- ²⁶⁾ P. K. Ghosh, *Introduction to Photoelectron Spectroscopy*, p. 179, John Wiley & Sons, New York 1983.
- ²⁷⁾ A. Schweig, W. Thiel, *J. Electron Spectrosc. Relat. Phenom.* **3** (1974) 27.
- ²⁸⁾ ^{28a)} J. M. Foster, S. F. Boys, *Rev. Mod. Phys.* **32** (1969) 300. — ^{28b)} M. Scholz, H. J. Köhler, *Quantenchemie*, vol. 3, p. 384, Dr. Alfred Hüthig Verlag, Heidelberg 1981. — ^{28c)} D. Pecters, *QCPE Nr. 330, Newsletter 57*, May 1977, p. 19.
- ²⁹⁾ R. D. Levin, S. G. Lias, *Ionization Potentials and Appearance Potential Measurements, 1971–1981*, Natl. Bur. Stand. (U.S.), U.S. Government Printing Office, Washington 1982.
- ³⁰⁾ F. Carnovale, T. H. Gan, J. B. Peel, A. B. Holmes, *J. Chem. Soc., Perkin Trans. 2*, **1981**, 991.
- ³¹⁾ H. D. Martin, M. Müller, B. Mayer, H. Haddad, A. Steigel, G. Distefano, A. Modelli, *Chem. Ber.* **119** (1986) 1613.
- ³²⁾ A. D. Bain, J. C. Bünzli, D. C. Frost, L. Weiler, *J. Am. Chem. Soc.* **95** (1973) 291.

[269/90]